Procedia Manufacturing

Volume 1, 2015, Pages 854–865

43rd Proceedings of the North American Manufacturing Research Institution of SME http://www.sme.org/namrc

Experimental Investigation of the Formability of Organic Coated Steel Sheet Metal

Holger Heinzel, Maziar Ramezani* and Thomas Neitzert
Auckland University of Technology, Auckland, New Zealand
heinzel.holger@gmail.com, maziar.ramezani@aut.ac.nz, thomas.neitzert@aut.ac.nz

Abstract
Application of the coating to material in a flat condition has economical, technological and ecological advantages. As the material is subsequently formed into shape not only the base material needs to withstand this process but the coating as well. Development of forming tools for coated metals is mainly concerned with the prediction of performance of the base material and does not analyse the condition of the coating. However, during the forming process, major surface damage can occur when the coated sheet is bent and unbent around the die geometry. To reduce surface damage of coatings, proper control of the parameters during forming and a detail study of the surface conditions is required. This research is conducted on metallically and organically coated sheet material which is commonly used for structural applications. The crack density of the coating is analysed during a deep drawing process and a forming limit diagram is obtained from the biaxial straining of the prepainted steel samples. The results show that cracks initiate from within the organic coating and are linked to the strain in the base material.

Keywords: Biaxial straining, Coating, Crack density, Forming limit diagram, Prepainted steel

1 Introduction

Press-forming is one of the most important manufacturing processes for fabricating sheet metal components. It is widely used for the mass production of small to medium size components. Industries like automotive, aircraft and whiteware are extensive users of the technology and the main drivers for new developments (Selles et al., 2012). Press forming is traditionally done on bare sheet metals which as such are prone to corrosion and are only of moderate aesthetic appeal (Carlsson et al., 2001). In order to combat these shortcomings coatings of organic and inorganic nature are applied to the material. Coatings require the substrate to have a highly cleaned surface, which can be difficult to achieve for pressed parts as not all areas enable easy access. The cleaning process requires additional

* Corresponding author.

Peer-review under responsibility of the NAMRI Scientific Committee
doi:10.1016/j.promfg.2015.09.075

equipment in the manufacturing plant and produces large amounts of contaminated waste water that needs to be taken care of (Aleksandrovic et al., 2011).

Organic coatings, also known as paints, usually need to be cured during which harmful substances so called volatile organic compounds (VOCs) are released. In the presence of sunlight these VOCs can react with nitrogen oxides to form ozone in the atmosphere, leading to health problems in humans and are damaging the vegetation (Vayeda and Wang, 2007). Various countries have strict legislations these days to control pollution from coating processes. For the manufacturer, this results in additional cleaning equipment to comply with legislation. Hence coating is not only a challenging process, especially for manufactured components but in general also quite costly (Lee et al., 2007).

A solution for this problem is to apply the coating prior to the manufacturing process while the material is still of flat shape and in coil form. This process, called coil-coating, is run continuously and is usually highly automated thus resulting in improved coating quality, e.g. uniform thickness and better adherence (Jeon et al., 2012). On the other side, once coated the material surface is more sensitive and requires to be protected from damage. This is especially problematic as the material needs to be formed into its final shape as required. The coating needs to survive the forming process without being damaged and further without severely changing its properties (Li et al., 2012). In recent years, it has become state of the art to use metallically pre-coated materials for press forming operations, even leading to a reduced need for lubrication. To date, the use of organically coated material has not yet found widespread use.

The design of press-forming tools relies on an accurate prediction of final part properties without the need to build costly and time-consuming try-out tools. The main focus of the forming analyses however has been the performance of the base materials and not that of the coating (Prosek et al., 2010). In order to advance the use of pre-coated materials and hence benefit from the advantages mentioned above it is necessary to predict the condition of the coating after a forming operation. Few publications appeared in literature about the formability of precoated sheet materials (see e.g. Jaworski and Schmid, 1999; Huang et al., 2001; Kim et al., 2002; Ueda et al., 2003; van den Busch et al., 2008; Moon et al., 2012; Behrens and Gaebel, 2013); however, most of them did not take into account a crack analysis of the coated layer.

This paper will investigate the failure behaviour and the formability limits of the coating of New Zealand made sheet metal material for loading conditions as they occur in press forming operations and enable the prediction of final part properties including those of the coating by experimental analysis. For this task, a material test is required that closely replicates the forming conditions and allows close observation of primary failure modes. Standard tests for mechanical material analyses usually do not assess the performance of the coating. In order to combat this shortcoming, suitable tests will be identified in the process and combined to assess the performance of the coating under different forming conditions. This will enable the general analyses of press forming operations for this and other materials.

2 Materials and Methods

The material investigated in this research is a structural steel produced from iron sand found along New Zealand's west coast. Such material is mainly used for exterior applications, like metal roofs and garage doors. The prepainted material comprises of a cold rolled sheet metal core, one layer of metallic coating and two layers of organic coating (Figure 1). The material is commonly formed by continuous roll-forming processes.

The base material is produced from titanomagnetite rich iron sand using rotary kilns to reduce the ore to metallic iron. The cold rolled material used for finish painted material is available in two grades G300 and G550, in which the number represents the guaranteed minimum yield strength for the material in MPa. The base material is produced in a range of thicknesses.

A metallic coating is applied in a continuous hot dip process and consists of 45% zinc and 55% aluminium. The nominal coating mass is 170gm/m^2 which corresponds to a coating thickness of 25µm respectively per side. The organic coating is applied via rollers to the metallically coated sheet metal in a continuous coil coating process. The coating is applied in liquid form and subsequently oven cured with the base metal reaching a peak metal temperature of 235°C. The material and coating used as well as the nominal thickness of different layers are given in Table 1.

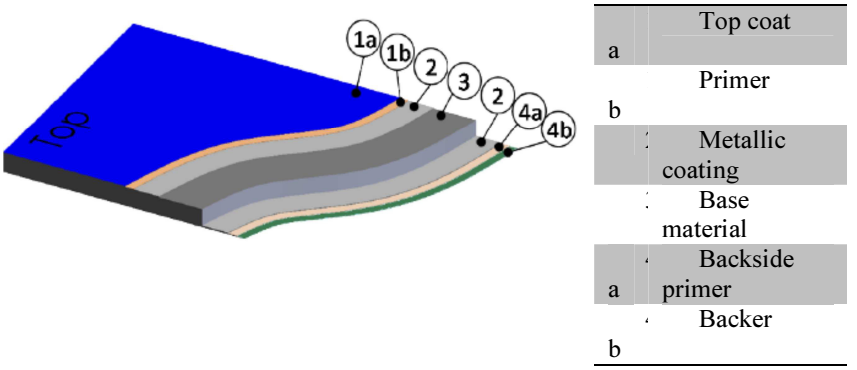

Figure 1: Layer composition of prepainted material.

Code	Material	Solvent	Use	Thickness [µm]
TA	Polyester	Solvent based	Top coat	17
TB	Acrylic	Water borne	Top coat	17
BA	Polyester	Water borne	Backer	10
PA	Polyester	Solvent based	Primer	6

Table 1: Organic coating specifications.

Prepainted material was used to deep draw round cups of 100mm diameter. This was done to confirm the principal suitability of the material for this kind of operation, to select the most suitable material, and to establish process parameters and limitations. Figure 2 shows a successfully drawn cup from prepainted material and the failures occurring in the organic coating at two locations. The images were taken without a scale under a light microscope. The forming-induced coating damage caused to the cup wall was visible to the unaided eye. The trials have confirmed that the G300 base material is better suited for deep-drawing operations than its higher strength counterpart where splitting is observed before a wall is properly formed. Further, the organic coating is found to deteriorate before failure occurs in the base material. Based on these results and the fact that standard production material is to be used for this research, G300 base material with 0.8mm thickness has been selected for all further investigations.

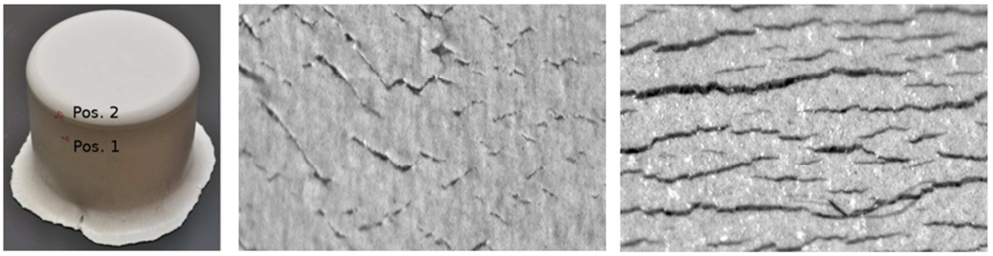

(a) (b) (c)

Figure 2: (a) Deep-drawn cup from prepainted material, (b) close-up of cracks in the coating at position1 and (c) position2.

Tensile samples have been cut from the material under different angles relative to the rolling direction (RD) of the material and tensioned under uniaxial load. As shown in Figure 3, the cracks that result from the straining appear transverse to the direction of loading and are not influenced by the orientation of the material and hence the cracking behaviour is assumed isotropic. Therefore, there are no anisotropy effects with respect to the organic coating, although the metal is not isotropic.

The mechanical analysis of the base material was performed on a Tinius Olsen benchtop tester equipped with longitudinal and transversal extensometers. Tensile test specimens with a gauge length of 80mm and a width of 20mm were employed as specified by ISO 6892. The biaxial straining was carried out on an Erichsen universal sheet metal testing machine. A hemispherical punch of 50mm diameter was used for the experiments. Throughout the testing, the surface strain was acquired with a visual strain measurement system from Vialux. The required surface marking were screen printed onto the laser cut specimen. The geometry of the specimens was designed with the shoulder section of the specimen ranging from 10mm to 75mm in order to achieve a wide range of strain combinations. All samples were taken from new stock material.

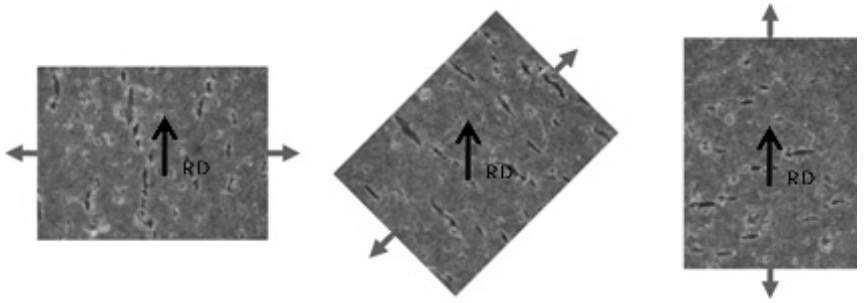

Figure 3: Crack orientations relative to the direction of force application, material samples aligned to rolling direction (RD).

Subsequent to the forming operation, the specimens were sectioned for surface examination using well lubricated cut-off equipment to limit heating of the specimen. The water-borne ink used for grid marking did not withstand the sectioning process to the effect that no strain measurement calibrations could be carried out on the surface images. Screen printing using water based ink was used to not damage the coating. Laser etching was considered, but the process damages the coating. Images of the surface were obtained with a Hitachi Scanning Electron Microscope without additional coating of the specimens. The SEM offers the advantage of a large depth of field compared to conventional microscopes which proved especially useful when imaging curved specimens. Energy of 1.0 keV at a distance of 16.2mm has shown not to alter the coating appearance. For the biaxial straining, two sets

of foils plus a thick layer of grease was used, while the samples were lightly oiled prior to deep drawing.

3 Results and Discussions

A typical punch force and blank holding force versus punch displacement are presented in Figure 4 for deep drawing of the 100mm diameter prepainted G300 steel sheet. In lubricated drawing tests a maximum drawing ratio of β_{max}=2.1 was established for this material as shown in Figure 5 using a punch velocity of 10mm/s at a temperature of 22ºC. The drawing ratio in the cylindrical drawing test is defined as $\beta=D_0/D_p$; where D_0 is the diameter of the steel sheet and D_p is the diameter of the punch.

Micrographic sectioning of uniaxially strained samples are used to identify the origin and depth of the appearing cracks. A total of ten samples are evaluated from two batches of material. The residual strain of the samples ranges from 5% to 20%. Figure 6 shows that cracks originate from within the organic coating and are not driven by cracks in the metallic coating. The coating has lower ductility than the substrate and when the sheet is stressed, the coating breaks giving rise to cracks in the coating. The bonding between the two organic coating layers and between the metallic coating and the organic coating are found not to be affected by the forming operations. The cross section of the cracks appears v-shaped, which is attributed to the contraction of the coating at the surface due to residual stress and local friction values and the remaining constraint at its base.

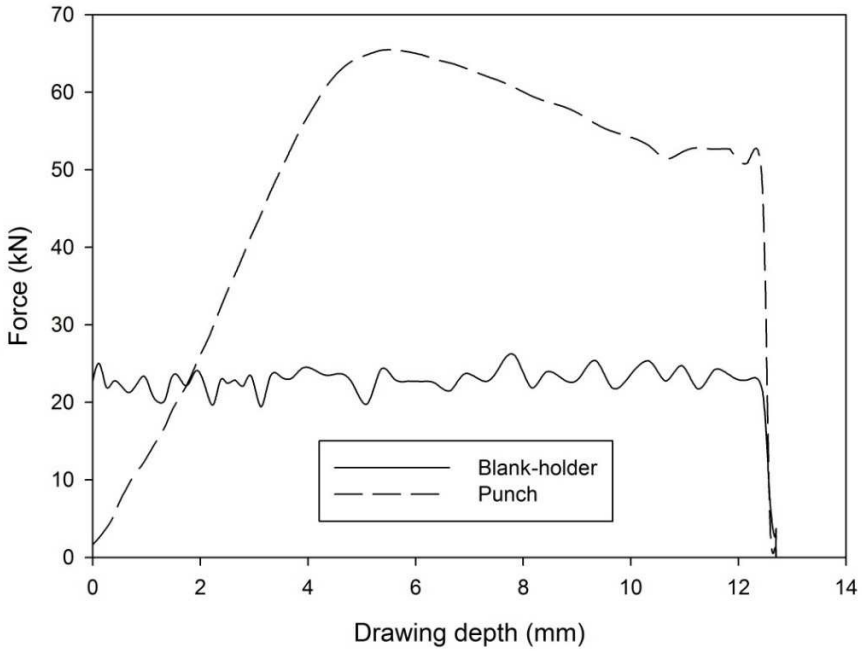

Figure 4: Typical punch force and blank-holder forces vs. drawing depth for deep drawing of G300 prepainted steel

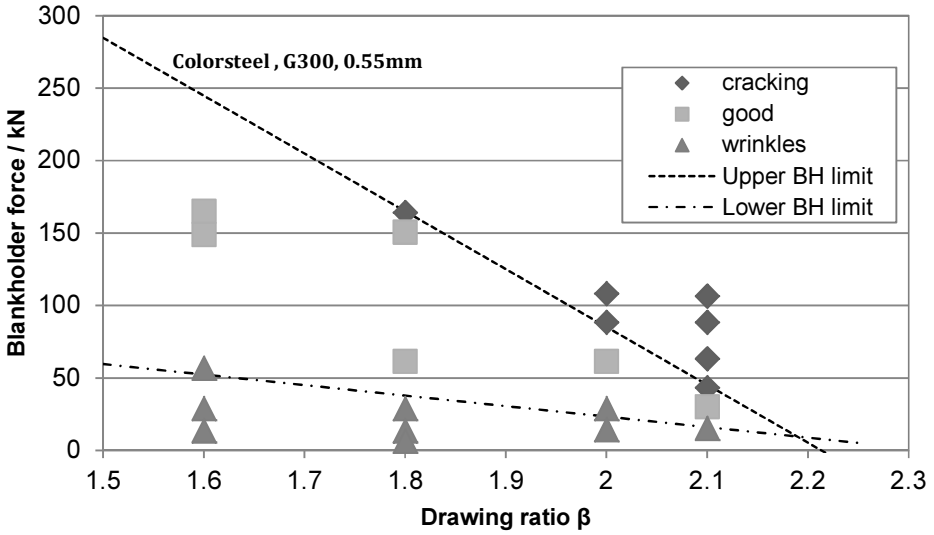

Figure 5: Determination of maximum drawing ratio $\beta_{max.}$

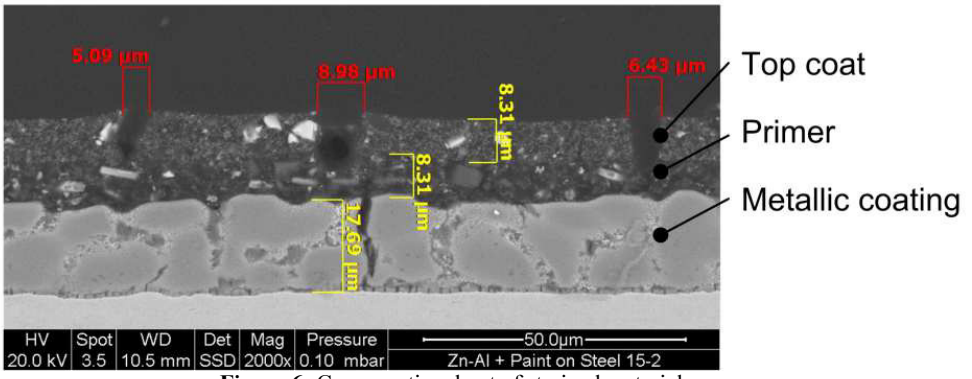

Figure 6: Cross-sectional cut of strained material.

The results of the tensile testing of the prepainted steel sheet are depicted in Table 2 and are averaged from three lots of testing. The material displays strong yielding characteristics with an observed yield elongation of up to 3%. Multiple necking sites could be observed within the parallel section of the test sample. The proof strength of 450MPa is found to be about 10% higher than the material's yield strength of 409MPa. Compared to the material properties of metallically coated material (σ_Y=335MPa, σ_U=425MPa) both values have increased considerably, although both materials comply with the strength specification for G300 material. The increase is presumed to result from the aging process during paint application. The values for uncoated material were supplied by the material manufacturer and are for fully aged material. The normal anisotropy of the material was taken at 10% elongation to account for an elongation at reaching proof strength at around 12%. Six tensile tests for organic coating samples were also conducted and the average elastic modulus of 2.198GPa was measured (Figure 7). Samples of organic coating have been prepared from the finish coated material by dissolving the metallic coating with hydrochloric acid.

Direction

Value		Unit	0°	45°	90°	Average
Strain hardening exp	n	-	0.145	0.137	0.140	0.141
Strength coefficient	K	MPa	689.12	689.80	678.62	685.40
Yield strength	σ_Y	MPa	403.55	406.36	416.97	409.46
Proof strength	σ_U	MPa	449.82	457.64	447.65	451.45
Elongation at σ_{Ue}	ε_m	-	0.123	0.118	0.120	0.120
Plastic strain ratio	r_{10}	-	1.146	1.002	1.251	1.140
Normal anisotropy	r_m	-				1.100
Planar anisotropy	Δr	-				0.196

Table 2: Summary of mechanical properties of prepainted material (G300, t=0.8mm).

Images of cross-sectioned samples as shown in Figure 6 can only be used to measure the distance between the opposing edges of a crack. The measured length depends on the orientation of the material relative to the cross-section, which is unknown and determinable at the time of measurement. Surface images, on the other hand, can be used to quantify the aerial size of the cracks and also contain information regarding the orientation of the faults relative to each other and also potentially relative to the sample. A major constraint for the coating is if it remains in good contact with the substrate. Crack formation has been used as a measure of integrity and protection of steel after forming. Tactile surface profiling equipment, as used for roughness measurements were trialed. The method had to be rejected as the needle was found to influence the examined coatings. A crack ratio C (crack density) is introduced to account for the severity of cracking. It is calculated from the total examined area S_t and the measured cracked area S_c as follows:

$$C = \frac{S_c}{S_t} \tag{1}$$

Typical images of strained samples received from the SEM are depicted in Figure 8 showing the appearance of the surface and cracks. The cracks appear to be of brittle nature, as expected from tensile tests carried out on the coating (Figure 7). The SEM produces greyscale images. The surface of most samples is found to exhibit a colour gradient across the images rather than a uniform colour. This is presumed to arise from the curved nature of the samples similar to images taken with a normal camera. Cracks appear brighter or darker than the surrounding material; often with one of the edges highlighted in a different colour. Crack area was calculated by using an automatic image analysis tool and MATLAB software.

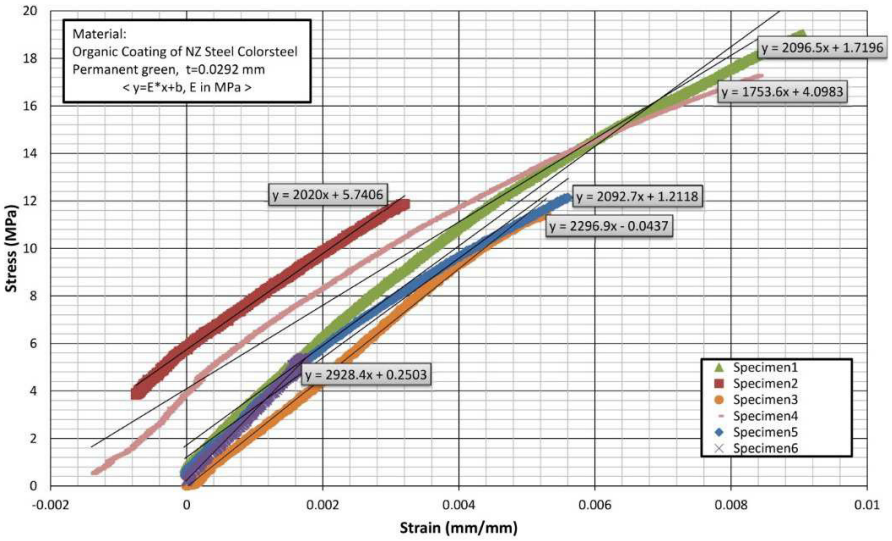

Figure 7: Tensile testing of organic coating (TB+PA).

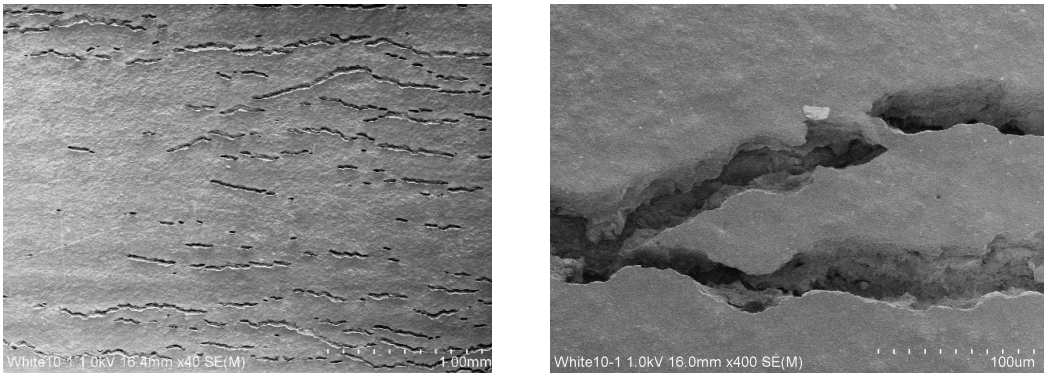

(a) (b)

Figure 8: Appearance of surface cracks in the organic coating at a magnification of (a) 40x and (b) 400x (Material TA).

Further experiments have been conducted to better understand the behaviour of individual material layers in the multilayer material. The interaction between the coating layers and the base material was researched using an Energy Dispersive Spectrometer (EDS). The material layers do not mix much as seen by the sharp changes in chemistry at the layer boundaries (Figure 9). As a result the material performance of the individual layers is expected to be similar to the behaviour of the individual material. An analysis of the fracture surface of the different material layers has been done to further compare the behaviour of single layer material and the multilayer setup of the prepainted sheet (Figure 10). During multiple cracking, individual coating cracks become arrested at the interface between the coating and substrate. Further loading of the sample causes additional cracks in the coating.

Figure 11 shows the crack density versus equivalent strain during uniaxial straining. It can be seen that the crack size and amount increase with increasing strain. Cracks start at around 5% equivalent strain in uniaxial straining. Crack density increases rapidly after the appearance of first coating crack. When the first crack forms, it will release the stresses in the coating near that crack surface and new

cracks will form immediately after the first crack forms. The cracks will continue forming until the cracks get close enough that their stress fields begin to interact.

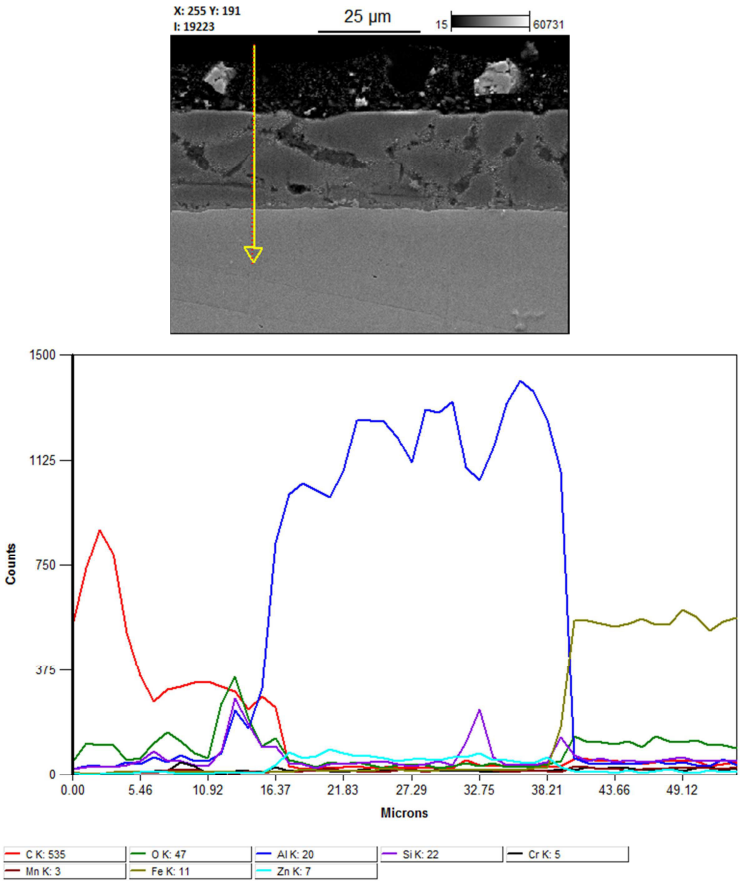

Figure 9: Chemical composition analysis of material sample across the coating using EDS.

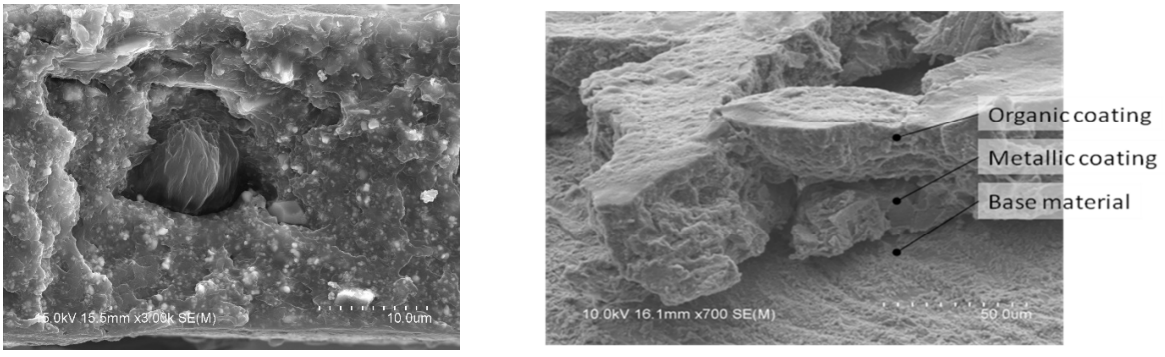

(a) (b)

Figure 10: Fracture surface of coating material. (a) 2-layer organic coating, (b) 2-layer organic and metallic coating atop finish coated sheet metal.

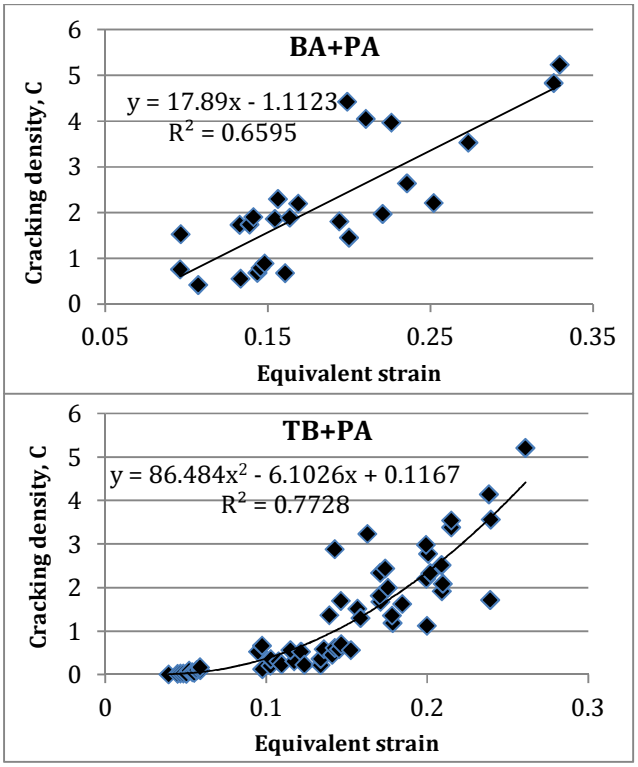

Figure 11: Crack densities vs. equivalent strain in the coating material.

During biaxial testing the surface strain is measured for the whole of the specimens using an inline visual strain measurement system and stored electronically. The local strain was measured using a printed surface grid. The specimens are formed up to a point where the base material starts to visibly fail. The local strain of the target area is averaged over 3 measurements representing an area of 4mm^2. The strain combination of the different samples is plotted in a forming limit diagram for coatings TA (Figure 12a) and TB (Figure 12b). The 9 major and minor strain values in each curve consist of the average values of three identical specimens each. The failure refers to the damage in the coating. Therefore, a coating-specific forming limit curve is defined in Figures 11 and 12 and can be used in the design of press-forming tools for precoated sheet materials and to forecast the occurrences of inacceptable coating damages and failure of base material.

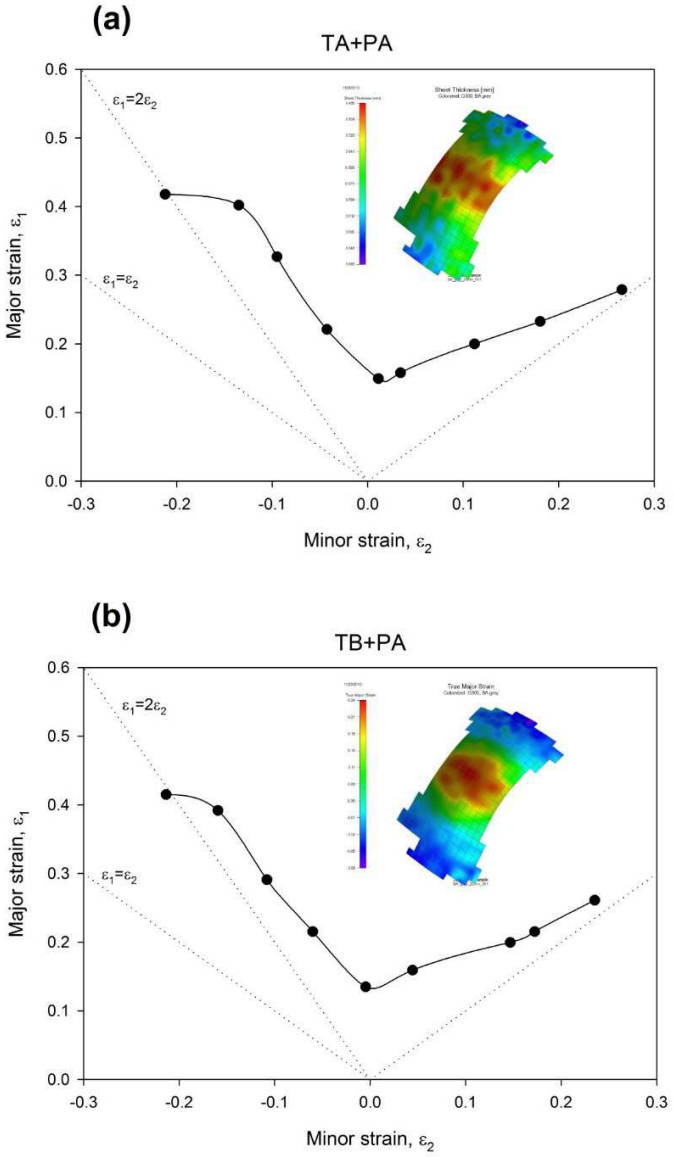

Figure 12: Forming limit diagram of G300 prepainted steel with coating material (a) TA and (b) TB.

4 Conclusions

Prepainted structural steel has successfully been drawn into cups. The coating has shown to deteriorate before the base material fails. The coating of the prepainted material exhibits fracture or cracking during the forming operation. This behaviour is used as performance criteria for the coating. The brittle fracture behaviour of the organic coating found in tensile testing correlates with the cracks in the coating observed in biaxial straining of the precoated sheet material. The coating has been shown to behave isotropic. The observed cracks have been found to originate from within the organic

coating and are linked to the strain in the base material. A biaxial tension state seems to have a greater effect on the organic coating than a mixed compression-tension state. The crack development of both top side organic coatings TA and TB is demonstrated to be similar. Local strain variations in the strained samples are observed and are attributed to the yield behaviour of the base material.

References

Aleksandrovic S, Stefanovic M, Adamovic D, Lazic V, Babic M, Nikolic R and Vujinovic T. Variable tribological conditions on the flange and nonmonotonous forming in deep drawing of coated sheets. *Journal of the Balkan Tribological Association* 2011; 17(2): 165-178.

Behrens BA and Gaebel CM. Formability of an anti-fingerprint clear coating on satin stainless steel sheet metal. *Production Engineering* 2013; 7(2-3): 275-281.

Carlsson P, Bexell U and Olsson M. Friction and wear mechanisms of thin organic permanent coatings deposited on hot-dip coated steel. *Wear* 2001; 247(1): 88-99.

Huang CH, Schmid SR and Wang JE. Thermal Effects on Polymer Laminated Steel Formability in Ironing. *Journal of Manufacturing Science and Engineering* 2001; 123:1-6.

Jaworski JA and Schmid SR. Survivability of Laminated Polymer Lubricant Films in Ironing. *Tribology Transactions* 1999; 42: 32-38.

Jeon YP, Seo HY, Kim JD and Kang CG. Experimental analysis of coating layer behavior of Al-Si-coated boron steel in a hot bending process for IT applications. *International Journal of Advanced Manufacturing Technology* 2013; 67(5-8): 1693-1700.

Kim HY, Hwang BC and Bae WB. An experimental study on forming characteristics of pre-coated sheet metals. *Journal of Materials Processing Technology* 2002; 120(1-3): 290-295.

Lee JM, Ko DC, Lee KS and Kim BM. Identification of the bulk behavior of coatings by nano-indentation test and FE-analysis and its application to forming analysis of the coated steel sheet. *Journal of Materials Processing Technology* 2007; 187-188: 309-313.

Li H, Chen J and Yang J. Experimental and numerical investigation of laminated steel sheet in V-bending process considering nonlinear visco-elasticity of polymer layer. *Journal of Materials Processing Technology* 2012; 212 (1): 36-45.

Moon JI, Lee YH and Kim HJ. Prediction of formability in drawing of PCM using tensile test and DMA creep test. *Polymer Testing* 2012; 31(4): 572-578.

Prosek T, Nazarov A, Olivier MG, Vandermiers C, Koberg D and Thierry D. The role of stress and topcoat properties in blistering of coil-coated materials. *Progress in Organic Coatings* 2010; 68(4): 328-333.

Selles MA, Schmid SR, Sanchez-Caballero S, Perez-Bernabeu E and Reig MJ. Upper-bound modelization of an ironed three-layered polymer-coated steel strip. *International Journal of Advanced Manufacturing Technology* 2012; 60(1-4): 161-171.

Ueda K, Kanai H and Amari T. Formability of polyester/melamine pre-painted steel sheets from rheological aspect. *Progress in Organic Coatings* 2002; 45(2-3): 267-272.

van den Bosch MJ, Schreurs PJG and Geers MGD. Identification and characterization of delamination in polymer coated metal sheet. *Journal of the Mechanics and Physics of Solids* 2008; 56(11): 3259-3276.

Vayeda R and Wang J. Adhesion of coatings to sheet metal under plastic deformation. *International Journal of Adhesion and Adhesives* 2007; 27(6): 480-492.